



Cite this: *Chem. Commun.*, 2020, 56, 2849

Received 28th December 2019,  
Accepted 30th January 2020

DOI: 10.1039/c9cc10028h

rsc.li/chemcomm

# A dual-ratiometric fluorescent probe for individual and continuous detection of H<sub>2</sub>S and HClO in living cells†

Xiuxiu Yue,<sup>‡a</sup> Jingpei Wang,<sup>‡a</sup> Jinliang Han,<sup>a</sup> Benhua Wang<sup>ID</sup>\*<sup>a</sup> and Xiangzhi Song<sup>ID</sup>\*<sup>ab</sup>

HClO and H<sub>2</sub>S are crucial for maintaining the homeostasis in cells and play vital roles in many physiological and pathological processes. Herein, we present a fluorescent probe that can respectively and simultaneously detect H<sub>2</sub>S and HClO in a dual-ratiometric manner with good linearity. Utilizing this probe, the imaging of intracellular H<sub>2</sub>S or/and HClO in living cells in a ratiometric manner was achieved.

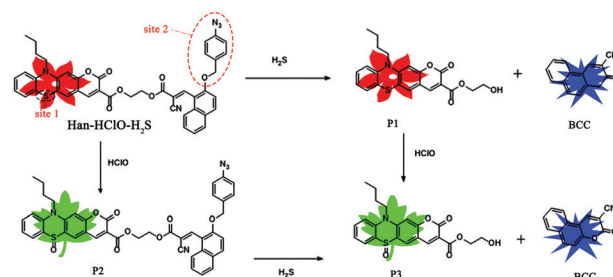
Hypochlorous acid (HClO), an important reactive oxygen species (ROS), possesses antibacterial activities and plays a vital role in killing pathogens and microorganisms.<sup>1</sup> HClO can be endogenously produced from hydrogen peroxide and chloride ions with the catalyzation of myeloperoxidase enzyme (MPO) in leukocytes.<sup>2</sup> A high level of intracellular HClO can cause serious tissue damage to induce a series of diseases, such as neurodegenerative diseases, atherosclerosis, cancer, ischemia, reperfusion injury, rheumatoid rheumatism, and so on.<sup>3</sup> Hydrogen sulfide (H<sub>2</sub>S), one of the important gaseous signaling molecules in organs and cells, has a prominent function in the human nervous system.<sup>4</sup> For example, it is validated that the roles of H<sub>2</sub>S in cardiovascular protection, vasodilation, cell growth, and neuromodulation are very important.<sup>5</sup> As a consequence, aberrant levels of H<sub>2</sub>S can lead to gastric mucosal injury, liver cirrhosis, Alzheimer's disease and other diseases.<sup>6</sup>

H<sub>2</sub>S and HClO have interplaying roles in many important physiological processes and are important mediators in brain function.<sup>7</sup> It is found that HClO causes extensive oxidative stress and oxidative damage in human neurodegenerative diseases.<sup>8</sup> *In vivo*, as a reducing agent, H<sub>2</sub>S serves as a specific HClO inhibitor for oxidative stress, cytotoxicity, protein

oxidation and lipid peroxidation.<sup>7a,8,9</sup> Therefore, the respective and continuous detection of H<sub>2</sub>S and HClO can help understand the interplay and cross-talk of these two species in cells.

Fluorescence techniques offer an attractive tool to monitor biological species with high spatial and temporal resolution in a noninvasive manner *in vivo*.<sup>10</sup> In the past decade, many efforts have been focused on the development of fluorescent probes to individually detect HClO or H<sub>2</sub>S.<sup>11</sup> To date, to the best of our knowledge, there are only two fluorescent probes reported to simultaneously detect HClO and H<sub>2</sub>S,<sup>11e,12</sup> both of which work in a turn-on manner. It is known that the ratiometric mode in fluorescence sensing is more desirable than the turn-on type due to the little interference from the background, minimized influences from instrumental factors, the concentration of the probe and other environmental factors.<sup>13</sup> Therefore, it is of great importance and a big challenge to develop a single-molecule fluorescent probe that can simultaneously detect HClO and H<sub>2</sub>S in a ratiometric manner.

Herein, a novel dual-ratiometric fluorescent probe, **Han-HClO-H<sub>2</sub>S**, was designed and synthesized for the discriminative detection of HClO and H<sub>2</sub>S respectively and continuously with good linearity (Scheme 1). Probe **Han-HClO-H<sub>2</sub>S** was obtained in five steps, as illustrated in Scheme S1, ESI.† As shown in Scheme 1, probe **Han-HClO-H<sub>2</sub>S** holds two reaction sites: (1) the phenothiazine moiety is sensitive to HClO; (2) the azide group



**Scheme 1** The proposed sensing mechanisms of probe **Han-HClO-H<sub>2</sub>S** for HClO, H<sub>2</sub>S and HClO/H<sub>2</sub>S with different fluorescence readouts.

<sup>a</sup> College of Chemistry & Chemical Engineering, Central South University, Changsha 410083, Hunan Province, China. E-mail: benhuawang@csu.edu.cn, song@rowland.harvard.edu

<sup>b</sup> Key Laboratory of Hunan Province for Water Environment and Agriculture Product Safety, Changsha 410083, Hunan Province, China

† Electronic supplementary information (ESI) available. See DOI: 10.1039/c9cc10028h

‡ These authors contributed equally to this work.

serves as a recognition group for  $\text{H}_2\text{S}$ . Probe **Han-HClO- $\text{H}_2\text{S}$**  was expected to fluoresce in the red spectral region. We hypothesized that the presence of HClO would oxidize the phenothiazine moiety in probe **Han-HClO- $\text{H}_2\text{S}$**  to largely decrease its electron-donating ability and thereby result in a fluorescence change from red to green, and ratiometric detection could be realized. With regard to  $\text{H}_2\text{S}$ , the azide group is expected to be reduced to form a blue fluorescent coumarin, while retaining the red-emitting phenothiazine coumarin, which can also afford a ratiometric fluorescence change to determine  $\text{H}_2\text{S}$ . If probe **Han-HClO- $\text{H}_2\text{S}$**  is treated with  $\text{H}_2\text{S}$  and HClO continuously, we expected that both recognition sites would be triggered to offer a mixed green-blue fluorescence. All in all, probe **Han-HClO- $\text{H}_2\text{S}$**  would sense  $\text{H}_2\text{S}$  or HClO and both through distinct fluorescence signal combinations.

Using a single molecule to sense two analytes respectively and simultaneously in a ratiometric manner, two specific reaction sites are at least needed. First, phenothiazine-coumarin was used as the fluorophore because of its red emission, fairly high fluorescence quantum yield, large Stokes shift and good photo-stability.<sup>14</sup> The sulfur atom (site 1) of phenothiazine-coumarin can be specifically oxidized by HClO to generate a green fluorescent coumarin. Second, we armed a precursor of blue-emitting coumarin with a  $\text{H}_2\text{S}$ -specific azide group (site 2). Once the azide group was reduced by  $\text{H}_2\text{S}$ , a blue-emitting coumarin **BCC** would be formed (Scheme 1). Finally, we conjugated these two above-mentioned moieties through an ester bond to obtain probe **Han-HClO- $\text{H}_2\text{S}$** , which would exhibit three kinds of ratiometric fluorescence changes for  $\text{H}_2\text{S}$  or HClO and both: red to red-blue for  $\text{H}_2\text{S}$ , red to green for HClO and red to green-blue for  $\text{H}_2\text{S} + \text{HClO}$ .

With probe **Han-HClO- $\text{H}_2\text{S}$**  in hand, we first investigated its optical properties toward  $\text{H}_2\text{S}$  and HClO in PBS buffer (10.0 mM, pH = 7.4) containing 50% acetonitrile, respectively. Probe **Han-HClO- $\text{H}_2\text{S}$**  exhibited a main visible absorption band centred at 450 nm (Fig. S1, ESI†). The addition of  $\text{H}_2\text{S}$  to the solution of probe **Han-HClO- $\text{H}_2\text{S}$**  caused negligible absorption changes. In contrast, the addition of HClO to the solution of probe **Han-HClO- $\text{H}_2\text{S}$**  blue-shifted the 450 nm band to 380 nm. Next, we turned our attention to the fluorescence behaviours of probe **Han-HClO- $\text{H}_2\text{S}$**  in response to  $\text{H}_2\text{S}$  and HClO (Fig. 1). Probe **Han-HClO- $\text{H}_2\text{S}$**  exhibited a red fluorescence with  $\lambda_{\text{max}}$  at 640 nm being excited at 440 nm. After the addition of  $\text{H}_2\text{S}$  to the solution of probe **Han-HClO- $\text{H}_2\text{S}$** , besides the stable red fluorescence, we observed a strong blue fluorescence with  $\lambda_{\text{max}}$  at 450 nm ( $\lambda_{\text{ex}} = 400$  nm). Qualitatively, the fluorescence changes of probe **Han-HClO- $\text{H}_2\text{S}$**  toward  $\text{H}_2\text{S}$  and HClO were in accordance with our expectation. To our delight, the red fluorescence signals exhibited an unchanged intensity before and after the addition of  $\text{H}_2\text{S}$  and could serve as a built-in reference for the ratiometric detection. It was seen that the fluorescence intensity ratio at 450 nm and 640 nm ( $I_{450}/I_{640}$ ) was proportional to the added concentration of  $\text{H}_2\text{S}$  (0.0–400.0  $\mu\text{M}$ ) (Fig. 1C), and the limit of detection was 26 nM based on signal to noise = 3. Under excitation at 440 nm, the fluorescence of probe **Han-HClO- $\text{H}_2\text{S}$**  displayed a green fluorescence with  $\lambda_{\text{max}}$  at 520 nm



Fig. 1 Fluorescence spectra of probe **Han-HClO- $\text{H}_2\text{S}$**  (5.0  $\mu\text{M}$ ) with different concentrations of  $\text{H}_2\text{S}$  (0.0–100.0 equiv.) for 120 min (A and B) and HClO (0.0–80.0 equiv.) for 10 min (D and E) with the excitation at 400 nm and 440 nm. (C) The linear relationship between  $I_{450}/I_{640}$  and the concentration of  $\text{H}_2\text{S}$ . (F) The ratio of  $I_{520}/I_{640}$  vs. the concentration of HClO; inset: the linear relationship between the ratio of  $I_{520}/I_{640}$  and the concentration of HClO.

in response to HClO. The fluorescence intensity ratio at 520 nm and 640 nm ( $I_{520}/I_{640}$ ) showed a good linear relationship with the concentration of HClO in the range of 50.0–300.0  $\mu\text{M}$  with a 17 nM limit of detection (Fig. 1F). These optical results indicated that probe **Han-HClO- $\text{H}_2\text{S}$**  could sensitively and quantitatively respond to  $\text{H}_2\text{S}$  and HClO with different fluorescence signal patterns in ratiometric manners, respectively.

Next, the fluorescence responses of probe **Han-HClO- $\text{H}_2\text{S}$**  toward both  $\text{H}_2\text{S}$  and HClO were investigated (Fig. 2). First, probe **Han-HClO- $\text{H}_2\text{S}$**  was treated with 100.0 equiv. of  $\text{H}_2\text{S}$  and then incubated with different concentrations of HClO. The addition of HClO induced a fluorescence enhancement at 520 nm, while the emission intensity at 450 nm remained



Fig. 2 Top row: fluorescence properties of probe **Han-HClO- $\text{H}_2\text{S}$**  (5.0  $\mu\text{M}$ ) successively treated with 100.0 equiv. of  $\text{H}_2\text{S}$  for 120 min and different concentrations of HClO (0.0–120.0 equiv.) for 10 min. Bottom row: fluorescence properties of **Han-HClO- $\text{H}_2\text{S}$**  (5.0  $\mu\text{M}$ ) successively treated with 80.0 equiv. of HClO and different concentrations of  $\text{H}_2\text{S}$  (0.0–100.0 equiv.). Left column: emission spectra; right column: plots of fluorescence intensity ratio vs. the concentrations of HClO and  $\text{H}_2\text{S}$ .  $\lambda_{\text{ex}} = 400$  nm.

unchanged, and the ratio ( $I_{520}/I_{450}$ ) versus the concentration of HClO (100.0–450.0  $\mu\text{M}$ ) exhibited a good linear relationship. Meanwhile, we observed a fluorescence change from red to red-blue and to green-blue during the successive addition of  $\text{H}_2\text{S}$  and HClO. In a reverse addition order (HClO first, followed by  $\text{H}_2\text{S}$ ), the further addition of  $\text{H}_2\text{S}$  in the presence of HClO triggered an obvious fluorescence enhancement at 450 nm, and we were very pleased that the ratio of  $I_{450}/I_{520}$  presented a linear-relationship with the concentration of  $\text{H}_2\text{S}$  (50.0–400.0  $\mu\text{M}$ ). The solution of probe **Han-HClO- $\text{H}_2\text{S}$**  underwent a fluorescence color change from red to green and to green-blue. Therefore, probe **Han-HClO- $\text{H}_2\text{S}$**  could continuously and quantitatively detect  $\text{H}_2\text{S}$  and HClO in dual-ratiometric manners, and the detection was not affected by the existence of each other.

The above optical studies were in good agreement with our proposed sensing mechanism. In order to obtain solid support for the sensing mechanism, compounds **3** and **5**, the derivatives of the two main segments in probe **Han-HClO- $\text{H}_2\text{S}$** , were prepared and their absorption and emission spectra in the absence/presence of  $\text{H}_2\text{S}$  and HClO were determined, respectively (Fig. S2 and S3, ESI†). Compound **3** absorbed at 330 nm and was nearly non-fluorescent. In the presence of  $\text{H}_2\text{S}$ , compound **3** displayed an emission at 450 nm with negligible absorption change. Compound **5** had an intense absorption band at 440 nm and fluoresced at 640 nm. When treated with HClO, compound **5** exhibited an absorption at 385 nm and strong fluorescence with a maximum at 520 nm. These results matched the optical behaviors of probe **Han-HClO- $\text{H}_2\text{S}$**  in response to  $\text{H}_2\text{S}$  or HClO and both very well. Moreover, mass spectral analysis was carried out to elucidate the mechanism (Figs. S21–23, ESI†). As shown in Fig. S21 (ESI†), the mass spectrum of the reaction mixture of probe **Han-HClO- $\text{H}_2\text{S}$**  with HClO had a peak at 802.1869, which was assigned to the corresponding product **P2** (Scheme 1). In the spectrum of probe **Han-HClO- $\text{H}_2\text{S}$**  with  $\text{H}_2\text{S}$ , the expected mass peaks (434.1011 and 248.0914) for the proposed reaction products **P1** and **BCC** were found (Fig. S22, ESI†). What is more, the mixture of probe **Han-HClO- $\text{H}_2\text{S}$**  with continuous addition of  $\text{H}_2\text{S}$  and HClO gave two mass peaks at  $m/z$  450.0944 and 248.0914, corresponding to **P3** and **BCC** regardless of the addition order (Fig. S23, ESI†). The mass spectral analysis and the optical studies forcefully supported our proposed reaction mechanisms (Scheme 1).

To verify its selectivity, we studied the optical responses of probe **Han-HClO- $\text{H}_2\text{S}$**  toward various biologically relevant species including NO, ONOO $^-$ ,  $\cdot\text{OH}$ ,  $^1\text{O}_2$ ,  $\text{O}_2^{2-}$ , ROO $^-$ ,  $t\text{-BuO}\cdot$ , Cys, Hcy, GSH,  $\text{Na}_2\text{S}_2\text{O}_3$ ,  $\text{Na}_2\text{S}_2\text{O}_5$ , NaCl,  $\text{NaNO}_2$ ,  $\text{SCN}^-$ ,  $\text{Na}_2\text{SO}_3$ , KI,  $\text{Na}_2\text{CO}_3$ , NaF,  $\text{ZnCl}_2$ ,  $\text{Na}_2\text{SO}_4$ ,  $\text{NaHCO}_3$  and  $\text{H}_2\text{S}_2$ . Only  $\text{H}_2\text{S}$  induced a remarkable fluorescence enhancement at 450 nm (Fig. 3A), whereas the fluorescence aroused by other interfering analytes was negligible even by extending the incubation time up to 100 min. Likewise, only HClO resulted in a strong fluorescence enhancement at 520 nm and a fluorescence decline at 640 nm (Fig. 3B). As expected, negligible fluorescence changes could be observed for other test species. As a result, it could be concluded that **Han-HClO- $\text{H}_2\text{S}$**  displayed good selectivity to  $\text{H}_2\text{S}$  and HClO.

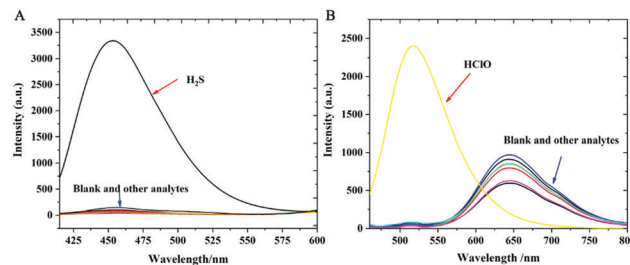


Fig. 3 Fluorescence spectra of probe **Han-HClO- $\text{H}_2\text{S}$**  (5.0  $\mu\text{M}$ ) in the presence of test species. (A)  $\text{H}_2\text{S}$ , Cys, Hcy, GSH,  $\text{Na}_2\text{S}_2\text{O}_3$ ,  $\text{Na}_2\text{S}_2\text{O}_5$ , NaCl,  $\text{NaNO}_2$ ,  $\text{SCN}^-$ ,  $\text{Na}_2\text{SO}_3$ , KI,  $\text{Na}_2\text{CO}_3$ , NaF,  $\text{ZnCl}_2$ ,  $\text{Na}_2\text{SO}_4$ ,  $\text{NaHCO}_3$  and  $\text{H}_2\text{S}_2$  (100.0 equiv. for each of them with 120 min incubation), excited at 400 nm; (B) HClO, NO, ONOO $^-$ ,  $\cdot\text{OH}$ ,  $^1\text{O}_2$ ,  $\text{O}_2^{2-}$ , ROO $^-$  and  $t\text{-BuO}\cdot$  (80.0 equiv. for each of them with 10 min incubation), excited at 440 nm.

In addition, the response kinetic profiles of probe **Han-HClO- $\text{H}_2\text{S}$**  toward  $\text{H}_2\text{S}$  and HClO were investigated (Fig. S5, ESI†). The addition of HClO to the solution of probe **Han-HClO- $\text{H}_2\text{S}$**  induced a dramatic enhancement in the fluorescence ratio ( $I_{520}/I_{640}$ ) within seconds. In the presence of  $\text{H}_2\text{S}$ , the fluorescence intensity ratio of  $I_{450}/I_{640}$  gradually increased and reached a plateau within about 70 min. As a control, the probe itself showed no fluorescence changes during the same time period.

In order to investigate whether **Han-HClO- $\text{H}_2\text{S}$**  has the ability to sense  $\text{H}_2\text{S}$  and HClO under physiological conditions, we then investigated the effect of pH on its fluorescence performance. The fluorescence of free probe **Han-HClO- $\text{H}_2\text{S}$**  remained unchanged within a wide pH range (Fig. S6, ESI†). In the presence of HClO or  $\text{H}_2\text{S}$ , the probe showed a striking enhancement in fluorescence ratio ( $I_{520}/I_{640}$ ) or ( $I_{450}/I_{640}$ ) within pH from 5.0 to 9.0, indicating that this probe was stable and could be used in physiological environments.

The attractive properties of probe **Han-HClO- $\text{H}_2\text{S}$**  in solution encouraged us to explore its capability to image the intracellular  $\text{H}_2\text{S}$  and HClO in cells. MTT assay on MCF-7 cells with probe **Han-HClO- $\text{H}_2\text{S}$**  indicated that it had a low cytotoxicity (Fig. S7, ESI†). Three channels (blue, green and red) were used to detect  $\text{H}_2\text{S}$  and HClO in living cells. Cells treated with probe **Han-HClO- $\text{H}_2\text{S}$**  gave off strong fluorescence in the red channel (Fig. 4d). When cells were pretreated with probe **Han-HClO- $\text{H}_2\text{S}$**  and then incubated with  $\text{H}_2\text{S}$ , strong fluorescence signals were observed from both the blue and red channels (Fig. 4g and i). The incubation of probe **Han-HClO- $\text{H}_2\text{S}$**  with HClO induced a striking fluorescence in the green channel (Fig. 4m). We then further tested the fluorescence behavior of probe **Han-HClO- $\text{H}_2\text{S}$**  with the continuous addition of  $\text{H}_2\text{S}$  and HClO in different orders in living cells. Probe-loaded cells were incubated with HClO for 20 min, washed with PBS buffer, and further treated with  $\text{H}_2\text{S}$  for another 1 h. As expected, intense fluorescence signals appeared from both the blue and green channels (Fig. 4q and r). When we changed the addition order of the two analytes, similar results could be seen (Fig. 4v and w). The above results demonstrated that probe **Han-HClO- $\text{H}_2\text{S}$**  could monitor intracellular  $\text{H}_2\text{S}$  or HClO and both through three different channels without interference from each other.





**Fig. 4** Bright field and fluorescence images of living MCF-7 cells. (a–e) Cells only treated with **Han-HClO-H<sub>2</sub>S** (5.0 μM) for 20 min. (f–j) Cells incubated with probe **Han-HClO-H<sub>2</sub>S** (5.0 μM) for 20 min and then treated with H<sub>2</sub>S (500.0 μM) for another 60 min. (k–o) Cells incubated with **Han-HClO-H<sub>2</sub>S** (5.0 μM) for 20 min and then treated with HClO (400.0 μM) for another 20 min. (p–t) Cells pre-treated with probe **Han-HClO-H<sub>2</sub>S** (5.0 μM) for 20 min, then incubated with H<sub>2</sub>S (500.0 μM) for 1 h, and further treated with HClO (600.0 μM) for 20 min. (u–y) Cells pre-treated with probe **Han-HClO-H<sub>2</sub>S** (5.0 μM) for 20 min, then incubated with HClO (400.0 μM) for 20 min, and further treated with H<sub>2</sub>S (500.0 μM) for 1 h. Blue channel: 420–500 nm (excited at 376 nm). Green channel: 515–580 nm (excited at 400 nm). Red channel: 570–650 nm (excited at 440 nm). Scale bar: 20 μm.

In summary, a fluorescent probe was developed to individually and continuously detect HClO or H<sub>2</sub>S and both for the first time in a ratiometric mode with high selectivity and sensitivity. In solution, this probe can qualitatively and quantitatively detect both H<sub>2</sub>S and HClO regardless of the addition order. Moreover, this probe was successfully applied to sense H<sub>2</sub>S or HClO and both in living cells with distinct fluorescence colors. The rational design strategy in this work holds potential to inspire the development of more powerful dual-response fluorescent probes for H<sub>2</sub>S/HClO and other biological molecules.

## Conflicts of interest

There are no conflicts to declare.

## Notes and references

- (a) P. Jia, Z. Zhuang, C. Liu, Z. Wang, Q. Duan, Z. Li, H. Zhu, B. Du, B. Zhu, W. Sheng and B. Kang, *Anal. Chim. Acta*, 2019, **1052**, 131–136; (b) Z. M. Prokopowicz, F. Arce, R. Biedron, C. L. L. Chiang, M. Ciszek, D. R. Katz, M. Nowakowska, S. Zapotoczny, J. Marcinkiewicz and B. M. Chain, *J. Immunol.*, 2010, **184**, 824–835.
- (a) T. Henrique de Araujo, S. S. Okada, E. E. B. Ghosn, N. N. Taniwaki, M. R. Rodrigues, S. Rogerio de Almeida, R. A. Mortara, M. Russo, A. Campa and R. C. Albuquerque, *Cell. Immunol.*, 2013, **281**, 27–30; (b) D. I. Pattison, C. L. Hawkins and M. J. Davies, *Chem. Res. Toxicol.*, 2003, **16**, 439–449.
- (a) C. L. Hawkins, D. I. Pattison and M. J. Davies, *Amino Acids*, 2003, **25**, 259–274; (b) Y. W. Yap, M. Whiteman and N. S. Cheung, *Cell. Signalling*, 2007, **19**, 219–228; (c) G. Li, Q. Lin, L. Sun, C. Feng, P. Zhang, B. Yu, Y. Chen, Y. Wen, H. Wang and L. Ji, *Biomaterials*, 2015, **53**, 285–295; (d) D. I. Pattison, C. L. Hawkins and M. J. Davies, *Chem. Res. Toxicol.*, 2003, **16**, 439–449.
- (a) H. Kimura, Y. Nagai, K. Umemura and Y. Kimura, *Antioxid. Redox Signaling*, 2005, **7**, 795–803; (b) B. L. Predmore, D. J. Lefer and G. Gojon, *Antioxid. Redox Signaling*, 2012, **17**, 119–140.
- (a) Y. Cai, L. Li, Z. Wang, J. Z. Sun, A. Qin and B. Z. Tang, *Chem. Commun.*, 2014, **50**, 8892–8895; (b) G. Yang, L. Wu, B. Jiang, W. Yang, J. Qi, K. Cao, Q. Meng, A. K. Mustafa, W. Mu and S. Zhang, *Science*, 2008, **322**, 587–590; (c) G.-J. Mao, T.-T. Wei, X.-X. Wang, S.-y. Huan, D.-Q. Lu, J. Zhang, X.-B. Zhang, W. Tan, G.-L. Shen and R.-Q. Yu, *Anal. Chem.*, 2013, **85**, 7875–7881.
- (a) S. Fiorucci, E. Antonelli, E. Distrutti, G. Rizzo, A. Mencarelli, S. Orlandi, R. Zanardo, B. Renga, M. Di Sante and A. Morelli, *Gastroenterology*, 2005, **129**, 1210–1224; (b) S. Fiorucci, E. Antonelli, A. Mencarelli, S. Orlandi, B. Renga, G. Rizzo, E. Distrutti, V. Shah and A. Morelli, *Hepatology*, 2005, **42**, 539–548; (c) K. Qu, S. Lee, J. Bian, C.-M. Low and P.-H. Wong, *Neurochem. Int.*, 2008, **52**, 155–165; (d) K. Eto, T. Asada, K. Arima, T. Makifuchi and H. Kimura, *Biochem. Biophys. Res. Commun.*, 2002, **293**, 1485–1488.
- (a) Y. Kimura, Y.-I. Goto and H. Kimura, *Antioxid. Redox Signaling*, 2010, **12**, 1–13; (b) L. A. Sena and N. S. Chandel, *Mol. Cell*, 2012, **48**, 158–167.
- J. K. Andersen, *Nat. Med.*, 2004, **10**, S18.
- M. Whiteman, N. S. Cheung, Y.-Z. Zhu, S. H. Chu, J. L. Siau, B. S. Wong, J. S. Armstrong and P. K. Moore, *Biochem. Biophys. Res. Commun.*, 2005, **326**, 794–798.
- B. N. Giepmans, S. R. Adams, M. H. Ellisman and R. Y. Tsien, *Science*, 2006, **312**, 217–224.
- (a) M. Ren, K. Zhou, L. He and W. Lin, *J. Mater. Chem. B*, 2018, **6**, 1716–1733; (b) X. Wu, Z. Li, L. Yang, J. Han and S. Han, *Chem. Sci.*, 2013, **4**, 460–467; (c) L. Yuan, L. Wang, B. K. Agrawalla, S.-J. Park, H. Zhu, B. Sivaraman, J. Peng, Q.-H. Xu and Y.-T. Chang, *J. Am. Chem. Soc.*, 2015, **137**, 5930–5938; (d) B. Deng, M. Ren, J.-Y. Wang, K. Zhou and W. Lin, *Sens. Actuators, B*, 2017, **248**, 50–56; (e) M. Ren, Z. Li, B. Deng, L. Wang and W. Lin, *Anal. Chem.*, 2019, **91**, 2932–2938; (f) B. Wang, P. Li, F. Yu, P. Song, X. Sun, S. Yang, Z. Lou and K. Han, *Chem. Commun.*, 2013, **49**, 1014–1016; (g) F. Liu, Y. Gao, J. Wang and S. Sun, *Analyst*, 2014, **139**, 3324–3329; (h) C. Zhang, Q. Nie, I. Ismail, Z. Xi and L. Yi, *Chem. Commun.*, 2018, **54**, 3835–3838; (i) X.-L. Liu, X.-J. Du, C.-G. Dai and Q.-H. Song, *J. Mater. Chem. B*, 2014, **79**, 9481–9489; (j) P. S. Zhang, X. Z. Nie, M. Gao, F. Zeng, A. J. Qin, S. Z. Wu and B. Z. Tang, *Mater. Chem. Front.*, 2017, **1**, 838–845; (k) Y. X. Hong, P. S. Zhang, H. Wang, M. L. Yu, Y. Gao and J. Chen, *Sens. Actuators, B*, 2018, **272**, 340–347; (l) Y. Huang, P. S. Zhang, M. Gao, F. Zeng, A. J. Qin, S. Z. Wu and B. Z. Tang, *Chem. Commun.*, 2016, **52**, 7288–7291; (m) J. Y. Ren, P. S. Zhang, H. Liu, C. H. Zhang, Y. Gao, J. X. Cui and J. Chen, *Sens. Actuators, B*, 2020, **304**, 127299; (n) D. L. Shi, S. Q. Chen, B. Dong, Y. H. Zhang, C. Q. Sheng, T. D. James and Y. Guo, *Chem. Sci.*, 2019, **10**, 3715–3722; (o) Y. H. Zhang, L. Ma, C. C. Tang, S. N. Pan, D. L. Shi, S. J. Wang, M. Y. Li and Y. Guo, *J. Mater. Chem. B*, 2018, **6**, 725–731; (p) Z. R. Lou, P. Li, Q. Pan and K. L. Han, *Chem. Commun.*, 2013, **49**, 1014–1016.
- X. Jiao, Y. Xiao, Y. Li, M. Liang, X. Xie, X. Wang and B. Tang, *Anal. Chem.*, 2018, **90**, 7510–7516.
- H. Xiong, L. He, Y. Zhang, J. Wang, X. Song and Z. Yang, *Chin. Chem. Lett.*, 2019, **30**, 1075–1077.
- (a) K. Kazlauskas, J. Mikulėnaitė, R. Karpicz, V. Gulbinas, J. Simokaitienė, A. Michalevičiūtė, J. Keruckas and J. Grazulevičius, *Dyes Pigm.*, 2009, **83**, 168–173; (b) L. Găină, I. Torje, E. Gal, A. Lupan, C. Bischin, R. Silaghi-Dumitrescu, G. Damian, P. Lönnecke, C. Cristea and L. Silaghi-Dumitrescu, *Dyes Pigm.*, 2014, **102**, 315–325; (c) H. Xiao, K. Xin, H. Dou, G. Yin, Y. Quan and R. Wang, *Chem. Commun.*, 2015, **51**, 1442–1445.